Jpn. J. Appl. Phys. Vol. 40 (2001) pp. 3231–3235
Part 1, No. 5A, May 2001

Electronic Structure Analyses of Sn-doped In_2O_3

Hidefumi ODAKA*, Yuzo SHIGESATO[1], Takashi MURAKAMI[2,†] and Shuichi IWATA[3]

Computer and Analysis Technology Center, Asahi Glass Co., Ltd., 1150, Hazawa-cho, Kanagawa-ku, Yokohama 221, Japan
[1]*College of Science and Engineering, Aoyama Gakuin University, 6-16-1, Chitosedai, Setagaya-ku, Tokyo 157, Japan*
[2]*Science and Technical Division, Teijin Molecular Simulations Inc., Hamacho-Hanacho Bldg. 4F, 2-17-8, Nihonbashi Hamacho, Chuo-ku, Tokyo 103, Japan*
[3]*RACE, The University of Tokyo, 4-6-1 Komaba, Meguro-ku, Tokyo 156, Japan*

(Received October 12, 2000; accepted for publication February 15, 2001)

Electronic structures of Sn-doped In_2O_3 (ITO) have been investigated for the first time by using a first-principles calculation method based on the density functional theory. Calculated partial density of states (PDOS) analyses showed that a Sn atom substituted for an indium one formed three impurity bands with s-like symmetry, the second band of the three bands overlapped the conduction band of In_2O_3, and the Fermi energy of ITO was captured in this impurity band. The PDOS analyses also revealed that the substitution of a Sn atom did not significantly destroy the shape of density of states around the bottom of the conduction band, which gave a physical foundation for the Burstein-Möss shift model used up to now. Carrier generation mechanism and past experimental results, such as those of X-ray photoelectron spectroscopy, temperature dependency of electrical conductivity and carrier-concentration dependency of optical effective mass of ITO, are discussed based on the present theoretical calculation results.

KEYWORDS: electronic structure, ITO

1. Introduction

Indium oxide (In_2O_3) with high dopant concentration of Sn (ITO) exhibits quasimetallic conductivity while maintaining its high transparency to visible light.[1)] Despite the fact that this interesting optoelectronic property has been widely applied[2)] in various technological products such as flat panel displays and solar cells, the physical mechanism responsible for the optoelectronic property has not been investigated in detail from the viewpoint of electronic structure. In particular, the electronic structures near the band gap which dominate the optoelectronic property have not been studied well theoretically and experimentally. One of the reasons for this appears to be that the complex unit cell of crystal In_2O_3 which contains 40 atoms had precluded a theoretical electronic structure calculation. Therefore the electronic structure was determined by experimental techniques such as X-ray photoelectron spectroscopy (XPS), from which, however, it was difficult to deduce the physical meaning of the spectroscopic data by itself.

Fan and Goodenough first suggested[3)] a schematic band-structure model which has been subsequently widely used and is still applied to account for known experimental properties of ITO. X-ray photoelectron spectroscopy analyses[4,5)] of In_2O_3 were performed to investigate the valence band structure directly, and revealed that the band width of the valence band was 6.0 eV or 6.8 eV and the band gap was 4.0 eV. The magnitude of this band gap was comparable to the direct band gap determined[1)] from the spectral absorption coefficient. The existence of an indirect band gap of about 2.6 eV was suggested.[6,7)] Bremsstrahlung isochromat spectroscopy (BIS) was used to analyze[5)] the conduction band of In_2O_3, which showed that the state density of the conduction band increased gradually with energy while that of the valence band rose abruptly below the edge of the valence band. This fact may be related to the light effective mass of electrons and the heavy mass of holes in In_2O_3, which was also suggested by the band gap widening studies of heavily Sn-doped In_2O_3.[1)] Recently, a theoretical band structure calculation has been performed[8)] for the crystal In_2O_3, which has clarified that the valence band is composed mainly of oxygen 2p-like states strongly hybridized with bonding indium-5s-like states and the conduction band consists mainly of antibonding indium-5s-like states with free-electron-like characteristics. This calculation also confirmed that the electronic structure calculation using a local density approximation could be used to analyze the overall features of XPS and BIS of In_2O_3 and could give physical meanings to these spectra.

In this study, the effect of substituting a Sn atom for an indium one on the electronic structure of In_2O_3 is analyzed using an augmented spherical wave (ASW) method[9)] with an atomic sphere approximation (ASA).[10)] This method has advantages, that is, it uses a minimum basis set and can be used to decompose the total density of states into a partial one. Therefore, this method is effective for the analyses of large systems and is useful for obtaining the physical features of materials. The purpose of this study is to investigate the roles of Sn atom in the optoelectronic properties of ITO based on first-principles calculation results.

2. Calculation Model and Method

As shown in Fig. 1, In_2O_3 crystallizes to form the bixbyite structure, with a space group symmetry of $Ia3$ and lattice constant of 10.117 Å. Conventional unit cell consists of 16 formula units of In_2O_3: the indium atoms occupy Wyckoff positions of 8b and 24d, and the oxygen atoms occupy Wyckoff positions of 48e. For practical electronic structure calculations, a primitive unit cell containing 40 atoms was used. For the analysis of Sn-doped In_2O_3 a primitive unit cell similar to that of In_2O_3 crystal was used: For the supercell calculation, one of the indium atoms at the 8b or 24d site was replaced by a Sn atom, which led to a system with a 2.5 at.% concentration of Sn, and approximately $1 \times 10^{21}/cm^3$ concentration of free electrons should have appeared if all the substituted Sn atoms had donated free electrons. Since

*E-mail address: odaka@agc.co.jp
†Permanent address: Business Planning and Development Science System Division, Teijin Systems Technology Ltd., 2-38-16 Hongo, Bunkyo-ku, Tokyo 113-0033, Japan.

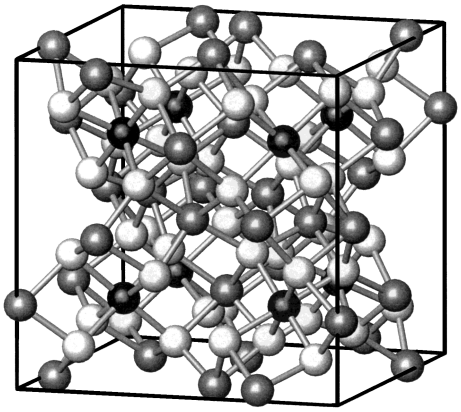

Fig. 1. Crystal structure of In_2O_3. Black, shaded and white spheres represent respectively 8b indium, 24d indium and 48e oxygen atoms in a conventional unit cell.

ITO films with very low resistivity are known to have about $1 \times 10^{21}/cm^3$ concentration of free electrons by some experimental methods,[11–13] this supercell model seems to be a good approximation of real ITO films with very low resistivity. In low resistivity ITO films prepared by the high-density plasma-assisted electron beam evaporation (HDPE) technique, the optimum concentration of Sn in In_2O_3 was approximately 0.7 at.%, and the resistivity and carrier concentration values were $2.8 \times 10^{-4}\,\Omega$cm and $5 \times 10^{20}/cm^3$, respectively.[11] For ITO films deposited by the spray technique, the optimum concentration of Sn atoms, resistivity and carrier concentration values were 9 at.%, $1.3 \times 10^{-4}\,\Omega$cm and $1.5 \times 10^{21}/cm^3$, respectively.[12] For ITO films deposited by the sputtering technique, the optimum concentration of Sn atoms depended on the experimental conditions and varied from 1 to 3 at.%, and the resistivity and maximum carrier concentration were around $1.0 \times 10^{-4}\,\Omega$cm and $1 \times 10^{21}/cm^3$, respectively.[13]

Electronic structure calculations were performed using the ASW method with ASA based on the density functional theory.[14] A first-principles software package called ESOCS[15] was used in this calculation. The exchange-correlation interaction was treated by the local density approximation using a parameterized form given by Hedin and Lundquist[16] and von Barth and Hedin.[17] Because the filling ratio of muffin-tin spheres to the interstitial region was small and the bixbyite structure has large interstitial spaces around 16c sites as shown in Fig. 2, empty spheres (ES) located at these sites were introduced to improve the calculation accuracy; One of the Wyckoff positions of ES was $x = 0.125$, $y = 0.125$, $z = 0.125$. The Wigner-Seitz radii of all atoms and ES were chosen to be 1.3702 Å. This treatment of the ASA was confirmed to be reliable by comparing the calculated results of In_2O_3 with the available experimental ones (see below). Relaxed core approximation was used from 1s to 4s states for indium and Sn, and to 2s states for oxygen. To construct the basis function for valence electrons, spherical harmonics components up to $l = 2$ for indium and Sn and up to $l = 1$ for oxygen and ES were used. In the analyses of In_2O_3, 7-k points in the irreducible first-Brillouin zone were used for determing the self-consistent charge density and 34-k points for calculating the partial density of states (PDOS). For ITO analyses, 32-k points in the first-Brillouin zone were used for determining self-consistent charge density and 500-k points to calculate the PDOS. A special point method proposed by Monkhorst and Pack[18] was used for these k-point samplings.

The band structure calculated for the crystal In_2O_3 is shown in Fig. 3, where the top of the valence band is chosen to be the zero of the energy scale. The conduction band exhibited a large dispersion and a significant free-electron-like characteristic around the Γ point. The effective mass of electrons in the conduction band was calculated by fitting its dispersion to a parabolic form. As a result, we obtained the value of $0.45m_e$ in the Γ–H direction, $0.32m_e$ in the Γ–N direction and $0.35m_e$ in the Γ–P direction, here, m_e is the rest mass of an electron. These results agreed well with the experimental results where the effective mass was estimated to be $0.3m_e$ by the plasma frequency analysis.[1,19] The calculated density of states (DOS) represented in Fig. 4 showed that the valence bandwidth of crystal In_2O_3 was 6.2 eV, which was close to that of the experimental data where the width was reported to be 6.0 eV or 6.8 eV.[4,5] Moreover, the features of the calculated DOS almost coincided with the experimental results of BIS and XPS.[4,5] Therefore, our calculation procedures were confirmed to be reliable for investigating the electronic structure of In_2O_3, except for the evaluation of band gap: The experimental band gap of In_2O_3 was about 4 eV[1,4,6] while the calculated one was 1.4 eV, which was due to the error from the local density approximation (LDA). The existence of an indirect gap was not confirmed by our calculation, which was consistent with the band structure calculation by the pseudopotential method.[20] In the following discussions of the Sn-doped In_2O_3 system, the same values of WS radii as those employed for In_2O_3 analyses were subsequently used for the supercell calculation including a Sn atom, whose sphere radius was chosen to be the same as that of indium.

3. Results and Discussions

In Fig. 4, the DOS is represented for a system in which a Sn atom is substituted for an indium atom at a 8b site in In_2O_3. Comparing the total density of states (TDOS) of this doped system with that of crystal In_2O_3, one can observe that the overall features of DOS corresponding to the valence and conduction of In_2O_3 are almost conserved except for the appearance of a new band below the valence band. The analysis of the PDOS shows that this band originates mainly from bonding states between Sn 5s-like and oxygen 2p-like states. The other two bands composed of *Sn* 5s-like states appear in the conduction band of In_2O_3 and slightly disturb this band, i.e., two antibonding bands with the Sn 5s-like characteristic exist in the conduction band and the Fermi energy is located in the lower band. Compared to the In 5s-like states of In_2O_3, the bonding band of Sn 5s-like state is located in the lower part in energy and the antibonding band is localized around the bottom of the conduction band. On the other hand, Sn 5p-like states generate two bands. The lower band hybridizes strongly with oxygen 2p-like states of In_2O_3, and the upper band lies in the conduction band. However, the contribution of Sn 5p-like states to TDOS around the Fermi energy is small compared with that of Sn 5s-like states in ITO. The authors had performed another electronic structure calculation in which the effect of a substitutional Sn atom for an indium one at a 24 d site was analyzed. Significant differences of electronic structures, however, were not found depending on

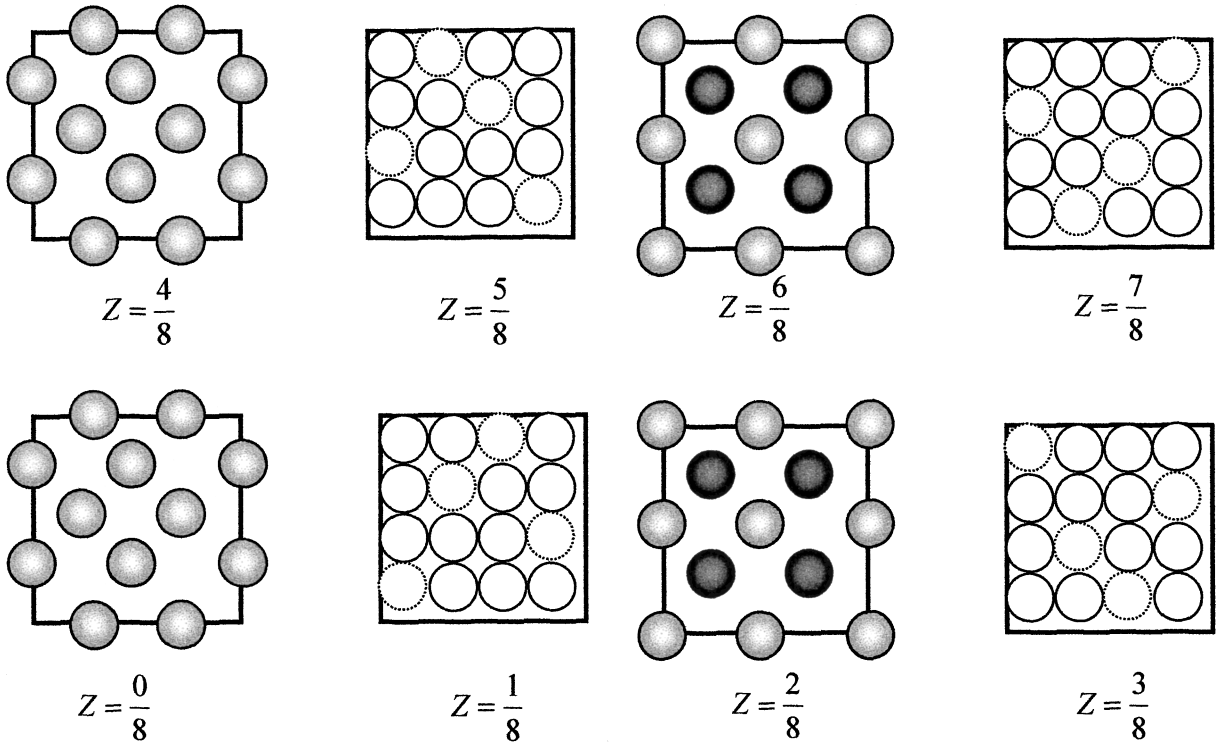

Fig. 2. Cross-sectional view[25] of unit cell of In_2O_3 along the z-axis is shown where ideal atomic positions are used to represent the atomic positions of In_2O_3 intelligibly. The 16c sites existed on the planes of $Z = 1/8$, 3/8, 5/8 and 7/8 on which ES at 16c sites is represented by a white sphere with a dotted line. The same symbol scheme as that of Fig. 1 was used to indicate the type of atoms.

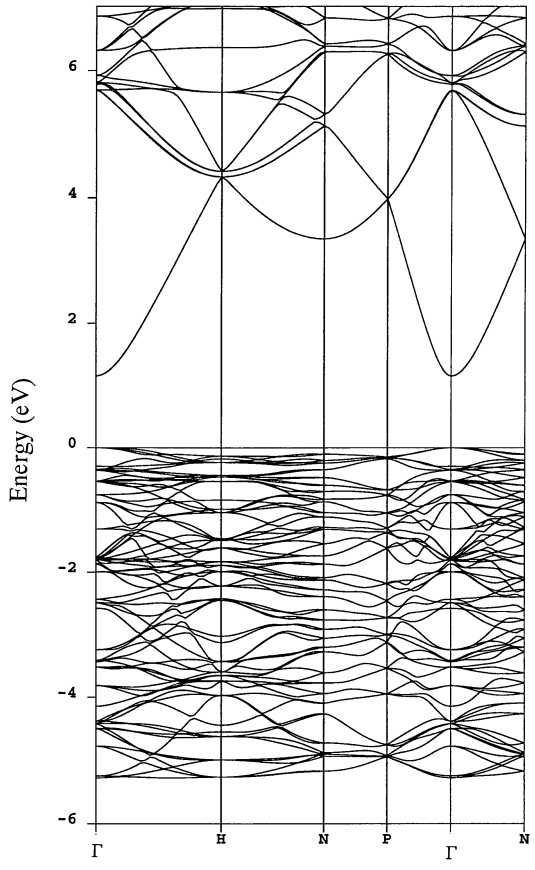

Fig. 3. Energy band structure of In_2O_3.

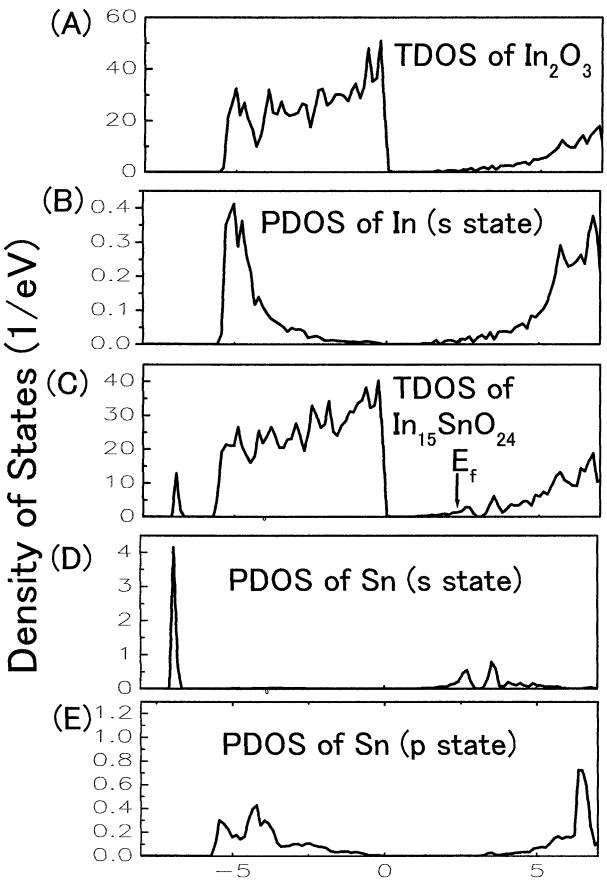

Fig. 4. Density of states analyses of $In_{15}SnO_{24}$.

the substitution site of the atom. Therefore, based on the calculated data for the system in which a substitutional Sn atom for an indium one at a 8b site exists, the authors will discuss the physical features of optoelectronic properties of ITO in

the following paragraph.

Since a Sn atom has one valence electron more than an indium atom, a substitutional Sn atom for an indium atom will be expected to donate one extra electron in ITO. Contrary to carrier generation phenomena observed in group IV semiconductors, since the concentration of impurities in the host crystal is very high, one can think of three scenarios for carrier generation in ITO. The first scenario is that Sn atoms donate their electrons to the conduction band of In_2O_3 which is constructed mainly from indium 5s-like states. In this case, the electrical conductivity is essentially due to the indium 5s-like conduction band and no additional energy such as light or heat to create carrier electrons is needed. The second scenario is that localized impurity bands exist below the conduction band and have a Sn-like character. In this instance, some energy will be needed to excite the electrons existing in the Sn-like state to the conduction band of In_2O_3, i.e., this physical feature gives a semiconductor-like behavior with an activation energy. The third scenario is that the donor band, i.e., the Sn-like state itself becomes the conduction band of ITO. In the analyses of Sb atoms in SnO_2,[21] the existence of such an impurity band was suggested.

In Fig. 4, antibonding Sn 5s-like states are observed to be located in the conduction band, and these states contribute almost one-fourth of the TDOS of ITO around the Fermi energy. The remainder of the TDOS is then covered by indium 5s-like and oxygen 3s-like states. Therefore an intermediate case between the first and the third scenario discussed above appears to occur in ITO, i.e., it is considered that a substitutional Sn atom donates an extra electron to the conduction band and this atom by itself forms a part of the conduction band along with the other atoms. Moreover, since the symmetry of the impurity state originated from the Sn atom is the same as that of the original state obtained from the replaced indium atom, i.e., both states are constructed from an anti bonding-like state with s-like symmetry, the original conduction band of In_2O_3 appears not to be disturbed significantly by this substitution and the TDOS of In_2O_3 appears to be approximately maintained around the Fermi energy. These factors dominate the chemistry between In_2O_3 and Sn to donate extra electrons efficiently without significantly disturbing the shape of the conduction band, i.e., without increasing the resistivity.

Band gap widening in ITO as a function of electron density is explained by a Burstein-Möss-shift model,[22,23] which is partially compensated by many body effects such as electron-electron and electron-impurity scattering.[1,19] In the above model, because of the lack of sufficient information regarding the band structures of In_2O_3 and ITO, the shapes of the conduction and valence bands around the band gap are assumed to be parabolic and independent of the Sn concentration. Our calculation showed that this assumption can be almost accepted as a description of both bands. As shown in Fig. 4, although a slight disturbance of the DOS corresponding to both bands is observed, the shape of these bands around the band gap is approximately retained independent of the substitution of Sn. This is because (1) most impurity states originating from a Sn atom do not exist around the band gap and (2) only the Sn's impurity states located in the conduction band have the same s-like symmetry as the that of conduction band.

The PDOS analyses discussed above can explain some past experimental results. In the studies of electrical properties of ITO, carrier density was investigated as a function of temperature using a Hall effect measurement technique, and it was determined that carrier density did not depend significantly on the temperature in the range 293 to 90 K.[24] This experimental result shows that an activation energy is not required to donate electrons in ITO, which is consistent with our calculation results. XPS spectra in the valence-band region are known to reflect the DOS. In a previous study,[32] the valence band spectra of ITO were studied for as-deposited and annealed ITO films. Then, ITO samples were found out to have only small structures near the Fermi energy, indicating that the density of states, $N(E_F)$, at the Fermi energy was small. Our calculation results show that the DOS around the bottom of the conduction band of In_2O_3 is not changed significantly by the substitution of Sn atoms and consists mainly of indium and Sn 5s-like states which have a small photoionization cross section[26–30] for X-rays. Therefore, it seems to be reasonable that $N(E_F)$ of ITO has a small structure and a Fermi edge is not clearly observed in the experiments. By using ITO samples prepared by the spraying method, the optical effective mass was found out to increase slightly with the carrier concentration.[31] Our calculation shows that the substitution of a Sn atom slightly disturbs the bottom of the conduction band of In_2O_3, which is observed as an increase of the optical effective mass.

4. Conclusions

In this study, a first attempt has been made to develop a coherent picture of the electronic structure of Sn-doped In_2O_3 by using the first-principles calculation method. As a result, it has become clear how a substituted Sn atom forms the impurity states in ITO where the Sn atom concentration is nearly the optimum for the formation of low-resisitivity ITO. Using the calculated energy band and DOS, we have provided a theoretical explanation of the experimentally observed results of this material.

1) I. Hamberg and C. G. Granqvist: Phys. Rev. B. **30** (1984) 3240.
2) C. G. Granqvist: *Materials Science for Solar Energy Conversion Systems* (Pergamon Press, Sweden, 1991).
3) J. C. C. Fan and B. Goodenough: J. Appl. Phys. **48** (1977) 3524.
4) T. L. Barr and Y. L. Liu: J. Phys. Chem. Solids **50** (1989) 657.
5) M. Orita, H. Sakai, M. Takeuchi, Y. Yamaguchi, T. Fujimoto, M. Fukumoto and I. Kojima: Hyomen Kagagu **17** (1996) 440 [in Japanese].
6) R. L. Weiher and R. P. Ley: J. Appl. Phys. **37** (1966) 299.
7) Y. Ohhata, F. Shinokai and S. Yoshida: Thin Solid Films **59** (1979) 255.
8) H. Odaka, S. Iwata, N. Taga, S. Ohnishi, Y. Kaneta and Y. Shigesato: Jpn. J. Appl. Phys. **36** (1997) 5551.
9) A. R. Williams, J. Kuebler and C. D. Gelatt: Phys. Rev. B **19** (1979) 6064.
10) O. K. Andersen: Phys. Rev. B **12** (1975) 3060.
11) Y. Shigesato, Y. Hayashi and T. Haranoh: Appl. Phys. Lett. **61** (1992) 73.
12) G. Frank and Kostlin: Appl. Phys. A **27** (1982) 197.
13) H. Kimura, H. Watanabe, S. Ishihara, Y. Suzuki and T. Ito: Shinku **16** (1987) 546 [in Japanese].
14) P. Hohenbergy and W. Kohn: Phys. Rev. **136** (1964) B864.
15) Esocs is a quantum mechanical software developed in Molecular Simulations Inc. (9685 Scranton Road San Diego, CA 92121-3752 U.S.A.)
16) L. Hedin and B. I. Lundquist: J. Phys. C **4** (1971) 3107.
17) U. von Barth and L. Hedin: J. Phys. C **4** (1972) 1629.
18) H. J. Monkhorst and J. D. Pack: Phys. Rev. B **13** (1976) 5188.
19) L. Gupta, A. Mansingh and P. K. Srivastava: Thin Solid Films **176**

(1989) 33.
20) Y. Mi, H. Odaka and S. Iwata: Jpn. J. Appl. Phys. **38** (1999) 3453.
21) K. C. Mishra, K. H. Johnson and P. C. Schmidt: Phys. Rev. B **51** (1995) 13972.
22) E. Burstein: Phys. Rev. **93** (1954) 632.
23) T. S. Möss: Proc. Phys. Soc. London Ser. B **67** (1954) 775.
24) Y. Shigesato and D. C. Paine: J. Appl. Phys. **73** (1993) 3805.
25) F. S. Galasso: *Structure and Properties of Inorganic Solids* (Pergamon Press, Oxford, 1970).
26) E. Storm and H. I. Israel: Nucl. Data Tables A **7** (1970) 565.
27) W. J. Veigele: At. Data **5** (1973) 51.
28) J. H. Scofield and J. Electron: Spectron Sectrosc. Relat. Phenom. **8** (1976) 129.
29) B. L. Henke, J. C. Davis, E. M. Gullikson and R. C. C. Perera: Lawerence Barkeley Lab. Rep., 1988, p. 26259.
30) J. J. Yeh and I. Lindau: At. Data & Nucl. Data Tables **32** (1985) 1.
31) R. Clanget: Appl. Phys. **2** (1973) 247.
32) N. Mori: J. Appl. Phys. **73** (1993) 1327.